

Nature-based shoreline protection by tidal marsh plants depends on trade-offs between avoidance and attenuation of hydrodynamic forces

Ken Schoutens^{b,*}, Maike Heuner^a, Elmar Fuchs^a, Vanessa Minden^e, Tilla Schulte-Ostermann^d, Jean-Philippe Belliard^b, Tjeerd J. Bouma^{c,f}, Stijn Temmerman^b

^a Department Ecological Interactions, Federal Institute of Hydrology, Germany

^b Ecosystem management research group, University of Antwerp, Belgium

^c NIOZ Royal Netherlands Institute for Sea Research, Department of Estuarine and Delta Systems, Yerseke, the Netherlands

^d Landscape Ecology Working Group, Carl von Ossietzky University of Oldenburg, Germany

^e Department of Biology, Ecology and Biodiversity, Vrije Universiteit Brussel, Belgium

^f Faculty of Geosciences, Utrecht University, Utrecht, the Netherlands

ARTICLE INFO

Keywords:

Tidal marshes
Wave attenuation
Flow attenuation
Shoreline protection
Trade-off

ABSTRACT

In face of growing land-flooding and shoreline-erosion risks along coastal and estuarine shorelines, tidal marshes are increasingly proposed as part of nature-based protection strategies. While the effect of plant species traits on their capacity to attenuate waves and currents has been extensively studied, the effect of species traits on their capacity to cope with and grow under wave and current forces has received comparatively less attention. We studied the relationships between species zonation and the associated two-way interactions between species traits and hydrodynamics, by quantifying the effectiveness of avoidance and attenuation of hydrodynamic forces under field conditions. Measurements were done for two pioneer tidal marsh species in the brackish part of the Elbe estuary (Germany). *Schoenoplectus tabernaemontani* (*S. tabernaemontani*), which grows as a single stem without leaves and *Bolboschoenus maritimus* (*B. maritimus*) which grows as a triangular stem with multiple leaves. Our results reveal that *S. tabernaemontani* grows more seaward being exposed to stronger hydrodynamic forces than *B. maritimus*. The stems of *S. tabernaemontani* have, in comparison to *B. maritimus*, a lower flexural stiffness and less biomass, which decrease the experienced drag forces, thereby favoring its capacity to avoid hydrodynamic stress. At the same time, these plant traits which favor such avoidance capacity, were shown to also result in a lower capacity to attenuate waves and currents. Hence this implies that there are trade-offs between avoiding and attenuating hydrodynamic forces. Most efficient attenuation of waves and currents is thus only reached when species have the ability to grow under the prevailing hydrodynamic forces. Therefore, we argue that the two-way interaction between plants and hydrodynamics contributes to species zonation. The presence of this species zonation in turn enhances the overall efficiency of nature-based shoreline protection in pioneer tidal marshes.

1. Introduction

Climate change increases the need for sustainable strategies to cope with projected sea level rise, increasing storm intensity, and associated growing risks of shoreline erosion and flooding of coastal and estuarine lowlands (Nicholls et al., 2008; Hallegatte et al., 2013; Woodruff et al., 2013; Tessler et al., 2015; Schipper et al., 2017). Additionally, regional to local human impacts have altered many estuarine and coastal landscapes. For example, dredging for navigation and conversion of natural floodplains into human land use protected by engineered flood defences

contribute to tidal wave amplification, which further increases the vulnerability of shorelines to flood and erosion risks (Pethick and Orford, 2013; Auerbach et al., 2015; Temmerman and Kirwan, 2015). In this context, it is increasingly proposed that conservation and restoration of natural ecosystems, such as tidal marshes, can provide a sustainable nature-based contribution to shoreline protection (Gedan et al., 2011; Temmerman et al., 2013; Bouma et al., 2014). Tidal marshes have the capacity to temporally store water, attenuate hydrodynamic forces and reduce erosion risks on more landward located human flood defences and infrastructures, even under extreme storm conditions (Möller

* Corresponding author.

E-mail address: ken.schoutens@uantwerpen.be (K. Schoutens).

<https://doi.org/10.1016/j.ecss.2020.106645>

Received 22 August 2019; Received in revised form 20 December 2019; Accepted 13 February 2020

Available online 21 February 2020

0272-7714/© 2020 Elsevier Ltd. All rights reserved.

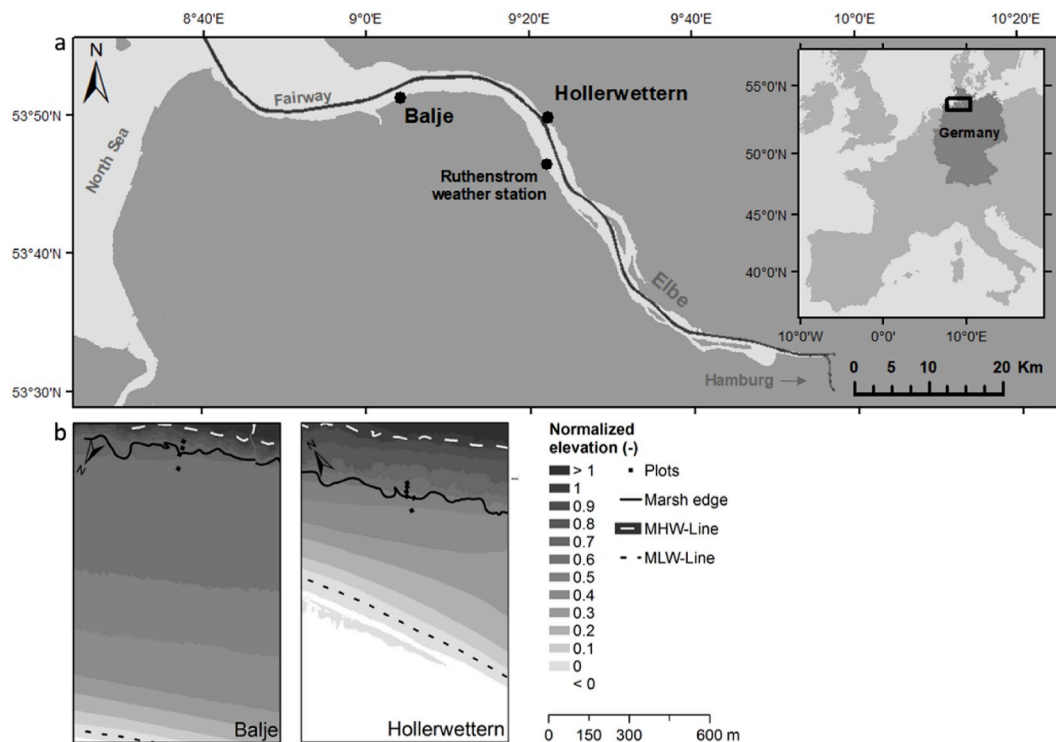


Fig. 1. Location of the Elbe estuary in Europe and of the study sites Balje and Hollerwetter (1a). The location of Ruthenstrom weather station is marked. The fairway (black line) goes to the harbour of Hamburg. The elevation maps for both sites show the measurement plots, the marsh edge and width of the tidal flat as well as the mean low and high water level (MLW and MHW). The elevations are normalized by tidal range as $(\text{Elevation} - \text{Mean low water}) / (\text{Mean high water} - \text{Mean low water})$ (1b).

et al., 2014; Stark et al., 2015; Vuik et al., 2016). In pioneer tidal marshes, which grow at the shoreward edge of marshes, friction induced by the physical presence of vegetation attenuates incoming hydrodynamic forces such as wave energy and current velocities. This well-studied mechanism shows that the majority of wave energy is reduced in the first meters of the pioneer marsh (Koch et al., 2009; Anderson and Smith, 2014). Wave heights can be reduced by 20–40% over 12 m of pioneer marshes (Silinski et al., 2017) and up to 80% over <50 m (Ysebaert et al., 2011) while current velocities can be reduced by more than 50% after 15 m (Nepf, 1999; Leonard and Croft, 2006; Tempest et al., 2015; Carus et al., 2016).

1.1. Plant strategies: avoidance versus resistance traits?

Plants in tidal marshes not only attenuate waves and currents, but they also have to cope with these incoming hydrodynamic forces. Mechanical stress from waves, currents and wind can alter the growth and survival of plant species (Biddington, 1986; Butler et al., 2012; Hamann and Puijalon, 2013; Schoelynck et al., 2015). Apart from waves and currents, plants in the intertidal area are exposed to wind generated mechanical stress during low water (Denny, 1994; Niels P. R. Anten et al., 2017). However in tidal marshes, the wind generated stress is relatively low compared to the stress generated by hydrodynamic forces (Denny and Gaylord, 2002). The main causes of mechanical plant failure by waves and currents are excessive drag forces acting on the plant shoots (Miler et al., 2012; Henry et al., 2015; Paul et al., 2016) and erosion (e.g. uprooting) around plants (Bouma et al., 2009; Friess et al., 2012). Nevertheless, plants developed adaptations to mitigate stress from drag induced by hydrodynamic forces. Morphological adaptations such as shape reconfiguration, compact size or simple architecture reduce or avoid drag (Sand-Jensen, 2003; Albayrak et al., 2012; Puijalon and Bornette, 2013), while increased rigidity or anchoring enables the plant to resist drag (Puijalon et al., 2008; Miler et al., 2012). Multiple

studies from different research fields point out a trade-off between the plant traits that favor an avoidance or a resistance strategy against mechanical stress (Puijalon et al., 2011; Anten and Sterck, 2012; Starko et al., 2015; Starko and Martone, 2016). This trade-off could have consequences for the growth, performance and ecology of a species (Denny et al., 2003; Puijalon and Bornette, 2013; Feagin et al., 2019). Moreover, growth strategies at the level of individual plants (i.e. plant traits) can thus have implications at the landscape scale for e.g. the shoreline protection capacity of a tidal marsh (Bouma et al., 2008, 2014; Vuik et al., 2016). However, studies on how species-specific marsh plant traits determine the plants' ability to cope with and survive hydrodynamic stress are rather sparse (Miler et al., 2014; Silinski et al., 2015, 2017).

1.2. Hydrodynamic avoidance VS attenuation capacity

Multiple studies have shown that the effectiveness of wave and flow attenuation within marshes is dependent on plant traits such as standing biomass, vegetation canopy height and stem stiffness, with higher, stiffer and denser vegetation canopies being more effective on flow and wave attenuation (Bouma et al., 2010; Callaghan et al., 2010; Paul et al., 2016; Rupprecht et al., 2017). Additionally, the species-specific capacity to avoid hydrodynamic stress was recently suggested to play a role in the spatial distribution (zonation) of two pioneer tidal marsh species in the wave-exposed parts of the brackish zone of NW European estuaries. More specifically, Heuner et al. (2018) showed that *Schoenoplectus tabernaemontani* (C.C.Gmel.) Palla is highly dominant in the pioneer zone, while *Bolboschoenus maritimus* (L.) Palla grows more landward at a farther distance from the marsh edge. Moreover, laboratory flume experiments, showed that plants sampled from the *Schoenoplectus*-zone had aboveground plant traits that favor avoidance of wave-induced stress: i.e., low frontal surface area and flexible stems, so that lower drag forces from waves were measured on the plants (Heuner et al.,

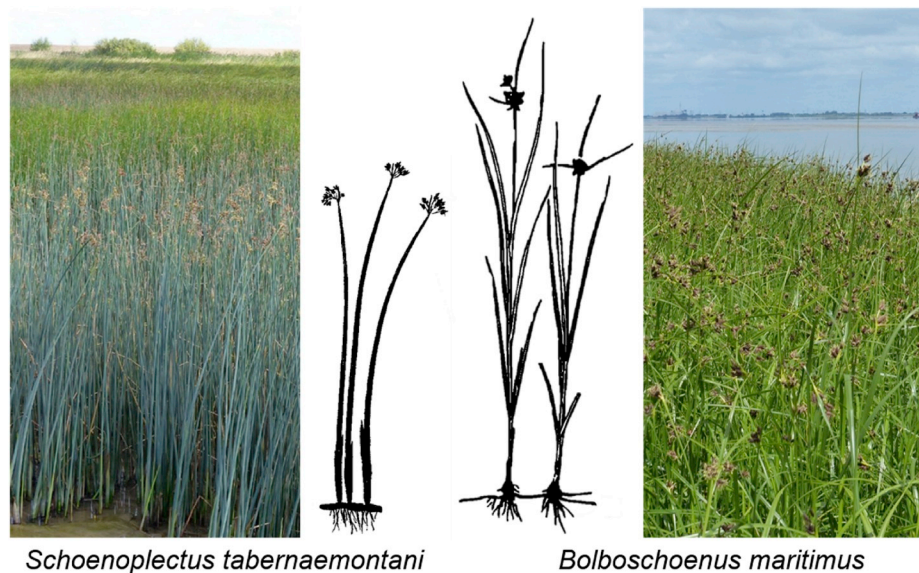


Fig. 2. Marsh vegetation of the brackish parts of the Elbe estuary is composed of two dominant pioneer marsh species: *Schoenoplectus tabernaemontani* (C.C.Gmel.) Palla which typically grows at the shoreward edge, and *Bolboschoenus maritimus* (L.) Palla which typically grows more landward.

2015; Silinski et al., 2016). In contrast, plants from the *Bolboschoenus*-zone had aboveground plant traits that result in less effective avoidance of wave-induced stress: i.e., higher stem surface area and stiffer stems, causing higher drag forces from waves. An additional flume experiment showed that wave attenuation rates were smaller for the more flexible plants sampled and grown from the *Schoenoplectus*-zone as compared to the stiffer plants from the *Bolboschoenus*-zone. Overall, these findings were interpreted as a cost-benefit trade-off as suggested in Bouma et al. (2005) for other intertidal plant species. They described a trade-off between stress-avoidance capacity (i.e. the more flexible species have a higher capacity to avoid wave-induced drag forces) versus ecosystem-engineering capacity (i.e. the more flexible species have less wave attenuation capacity). We emphasize here that these findings are based on experiments in laboratory flumes, where both species are exposed to similar wave conditions. In the field, however, both species grow in sequential zones, and hence most likely experience different physical forcing from waves and currents. This raises the question how a trade-off between stress-avoidance capacity versus ecosystem-engineering capacity applies to *in-vivo* field conditions, accounting for the fact that each species has its own unique habitat. We further hypothesize that similar plant traits are responsible for both the ability to grow under hydrodynamic forces and the capacity to attenuate these hydrodynamic forces.

In this study, we aim to further deepen our insights into the two-way interaction between plant traits and hydrodynamics, by *i*) relating the observed plant species zonation to field measurements of species-specific traits and physical forcing by waves and currents in the different zones and *ii*) analyzing how these species-specific traits imply trade-offs between the effectiveness of hydrodynamic-stress-avoidance vs. attenuation of hydrodynamic forces. To our knowledge, there is no literature that discusses the implications of this trade-off for the attenuation capacity of hydrodynamic forces (and hence for nature-based shoreline protection capacity) of pioneer tidal marshes.

2. Methods

2.1. Study sites

Two sites were selected along the brackish part of the Elbe estuary, Germany: Balje (53°51'23.5"N, 9°49.2"E) and Hollerwetterm (53°49'55.5"N, 9°22'17.4"E) (Fig. 1a). These two sites are characterized

by a gentle transition between bare tidal flat and marsh, and a spatial zonation of plant species (see section 'Studied species' below) growing in distinct zones that run parallel to the estuarine tidal channel (Fig. 1b). The semidiurnal tide is on average 2.8 m (1.6 m during neap tide and 3.8 m during spring tide, data for 2015–2017). Mean freshwater discharge of the Elbe (1926–2014) is $712 \text{ m}^3 \text{ s}^{-1}$ ranging from $560 \text{ m}^3 \text{ s}^{-1}$ in summer to $866 \text{ m}^3 \text{ s}^{-1}$ in winter (Strotmann, 2014). The water salinity measured using the Practical Salinity Scale at the two sites ranges between 0.3 and 4.0.

2.2. Studied species

Along the brackish parts of NW European estuaries *Schoenoplectus tabernaemontani* (C.C.Gmel.) Palla (formerly *Scirpus tabernaemontani*) and *Bolboschoenus maritimus* (L.) Palla (formerly *Scirpus maritimus*), both members of the Cyperaceae-family, are the most common pioneer plant species. In tidal marshes, both species typically reproduce by clonal outgrowth resulting in rhizomatous root networks. In winter the aboveground biomass of both species dies off and is flushed away while the roots hibernate (Schoutens et al., 2019). *S. tabernaemontani* shoots grow as single stems with a circular cross-section, a diameter around 15 mm, and a height up to 2.0 m (own measurements) (Fig. 2). At the base there are a few small leaf sheaths embracing the round stem. In contrast, *B. maritimus* has leaves along the full length of a triangular stem that can grow up to 2.5 m in height and have a base length of the triangular cross-section up to 17 mm (own measurements). Both species form dense monospecific zones in belts that run parallel to the marsh edge. They both grow at overlapping elevations relative to mean sea level in which *S. tabernaemontani* typically grows directly adjacent to the shoreward edge of marshes, while *B. maritimus* grows in a more landward located zone (Heuner et al., 2018).

2.3. Overall description of the field measurements

This study investigated how species zonation is determined by the two-way interaction of plant traits and hydrodynamic forces. The resulting trade-offs between the effectiveness of avoidance and attenuation of hydrodynamic forces were assessed under field conditions. First, the spatial distribution in terms of species zonation was illustrated using maps of the Elbe estuary. Next, the hydrodynamic conditions acting upon the two species (i.e. exposed or sheltered from waves and currents)

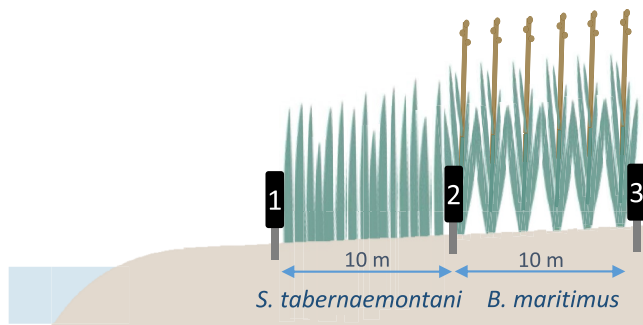


Fig. 3. Schematic cross section of the field monitoring setup. Along the sea-to-land transect sensors were installed at 3 locations to measure hydrodynamic conditions (waves and currents). Wave attenuation was measured over a 10 m vegetation belt between sensor 1 and sensor 2 for *S. tabernaemontani* and between sensor 2 and 3 for *B. maritimus* vegetation. Flow velocities were measured in a similar way but only at site Hollerwetterm. Plant traits were measured in every respective species zone.

were measured locally at the two study sites throughout the growing season with wave height and current velocities as proxies. These measurements were accompanied by quantification of wave and flow attenuation rates per species zone to illustrate their capacity to attenuate hydrodynamics at peak biomass. We then coupled the two way interactions with field measurements of species-specific plant traits that play a role in the interaction with the hydrodynamics. Therefore, aboveground biomass, flexural stiffness and frontal plant area were used as proxies for drag forces exerted on the plant shoots (Vogel, 1996; Silinski et al., 2016). Combining these measurements allowed us to construct a conceptual mechanism of how species-specific plants traits play a key role in the spatial distribution of pioneer marsh plant species and what the consequences for nature-based shoreline protection might be.

2.4. Plant zonation

The frequency distribution of surface elevations at which both species are growing, was quantified for both study sites. This was compared to a similar analysis for all marshes in the Elbe estuary, see Fig. 1a), to demonstrate that the elevation range of both species in our two study sites is representative for what is generally found in the Elbe estuary. The analysis was based on vegetation maps, aerial pictures and digital elevation models (DEM) made in summer 2016. The vegetation maps were generated from aerial pictures (0.20 m resolution) (WSA, 2017). In both estuaries, 140 random sampling points were generated of which the elevation above MHW was extracted from the DEM (1.0 m grid and 0.5 m position accuracy) (Zentrales Datenmanagement der GDWS Standort Kiel, 2017). For more details on this method, we refer to Heuner et al., (2018). The elevations were normalized by tidal range as $(\text{Elevation} - \text{Mean low water}) / (\text{Mean high water} - \text{Mean low water})$, in order to be comparable between the datasets for the two sites and the whole Elbe estuary.

2.5. Plant exposure to and attenuation of hydrodynamic forces

2.5.1. Waves

During a six-month field campaign in the growing season from May to October 2016, wave heights were measured. Automated pressure sensors (P-Log3021-MMC, Driesen & Kern) were deployed at three distances along one cross-shore transect at every site (i.e. 2 x 3 sensors; Fig. 3) to record absolute pressure at 8 Hz. The 1st sensor was placed in front of the marsh edge for measuring incoming waves just before they enter the marsh vegetation. The 2nd sensor was placed at 10 m distance from the marsh edge, coinciding with the transition from the

S. tabernaemontani zone to the *B. maritimus* zone. Together with sensor 1, this set-up enabled quantifying wave attenuation over 10 m of *S. tabernaemontani* marsh. A third sensor was placed another 10 m further within the *B. maritimus* vegetation. Comparing sensor 2 and 3 allowed quantification of wave attenuation over 10 m of *B. maritimus* marsh.

To quantify wave heights, pressure data were converted into water surface elevation using a Matlab routine. After correction for atmospheric pressure (obtained from the DWD Climate Data Center, 2019), the resulting water levels were then corrected for depth-dependent pressure attenuation based on the linear wave theory (Dalrymple and Dean, 1991), i.e. the water motion of passing waves and hereby the hydrostatic pressure is attenuated with increasing water depth. Next, the tidal signal was extracted from the wave signal using a low-pass filter and zero-down crossing method was then applied on the resulting time series of wave fluctuations to determine individual waves (Vanlierde et al., 2011; Belliard et al., 2019). Significant wave height (H_s , mean of the highest third of recorded waves) and maximum wave height (H_{max} , mean of the 99th percentile of recorded waves) were calculated over 10 min time intervals. The relative wave attenuation rate (R_w) was calculated for *S. tabernaemontani* as $R_w = (H_1 - H_2) / H_1 \times 100(\%)$ where H_1 is the incoming significant wave height at sensor location 1 at the seaward edge of the vegetation zone and H_2 is the significant wave height at 10 m into the *S. tabernaemontani* zone. Similarly, the relative wave attenuation rate (R_w) was calculated for *B. maritimus* as $R_w = (H_2 - H_3) / H_2 \times 100(\%)$ where H_3 is the significant wave height at 10 m into the *B. maritimus* zone. For comparison with plant traits, the wave attenuation capacity was calculated during the period of peak biomass. With increasing water depth, the inundated frontal area of the plants increases and consequently the interaction of the waves with the vegetation increases until the water depth exceeds the canopy height. Since both species are growing at different surface elevations, wave attenuation rates were calculated and compared for water depth classes of 0.25 m intervals to enable a species comparison. A similar comparison between wave attenuation rates and wave height classes of 0.1 m intervals was made to take into account the wave transformation in front of the respective vegetation zone.

2.5.2. Flow velocity

As sensor availability was limited, flow velocities were only measured at Hollerwetterm during the growing season from May to October 2016 (Figs. 1 and 3). Next to the pressure sensors, flow velocities were measured at 4 Hz with ADVs (Acoustic Doppler Velocity sensors, Nortek) measuring at 0.10 m above the sediment bed. Raw data were removed for beam correlations below 70% after which the planar velocity (m/s) was calculated as $U = \sqrt{u^2 + v^2}$ with u and v being the mean flow velocities (m/s) in the two horizontal dimensions perpendicular to each other calculated over 10 min time intervals. Flow attenuation rate (R_f) was calculated similarly to the wave attenuation rate (see above: $R_f = (U_1 - U_2) / U_1 \times 100(\%)$ and $R_f = (U_2 - U_3) / U_2 \times 100(\%)$ respectively with U_1 , U_2 and U_3 are now mean flow velocities instead of wave heights at the respective measurement locations).

2.6. Plant traits

Quantification of species-specific plant traits was conducted at peak biomass in August 2016. Based on a literature study, we selected to focus on the principal plant traits responsible for (i) avoiding mechanical stress from waves and currents (e.g. Puijalon et al., 2011; Henry et al., 2015; Paul et al., 2016; Silinski et al., 2016; Chen et al., 2018) and (ii) the capacity to attenuate hydrodynamic forces. These plant traits can be grouped into shoot morphological traits (i.e., aboveground biomass density and frontal shoot area) and stem biomechanical traits (i.e., Young's modulus and flexural stiffness) (e.g. Bouma et al., 2010; Anderson et al., 2011; Shepard et al., 2011; Vuik et al., 2016; Rupprecht

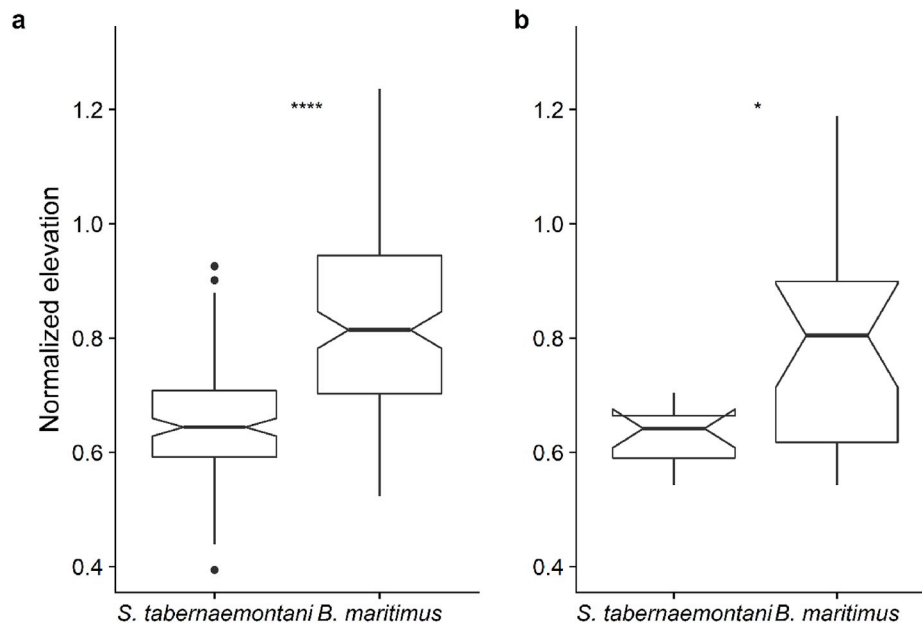


Fig. 4. The elevation niche of both *B. maritimus* and *S. tabernaemontani* for (a) the Elbe estuary ($n = 140$ for both *S. tabernaemontani* and *B. maritimus*) and (b) for the study plots Balje and Hollerwettern ($n = 12$ for *S. tabernaemontani* and $n = 24$ for *B. maritimus*). The elevations are normalized by tidal range as $(\text{Elevation} - \text{Mean low water}) / (\text{Mean high water} - \text{Mean low water})$. Significance of differences was tested with the non-parametric Wilcoxon test (**** represents $p < 0.001$).

et al., 2017; Silinski et al., 2017; Schulze et al., 2019).

2.6.1. Plant morphological traits

Shoot densities were determined per species by counting the number of shoots within three permanent quadrats of $0.4 \text{ m} \times 0.4 \text{ m}$. Above-ground biomass of both species was sampled by clipping all shoots in a $0.2 \text{ m} \times 0.2 \text{ m}$ quadrat (if needed this was repeated until a minimum of 20 shoots was reached). Above-ground biomass density (kg/m^2) was quantified by multiplying counted shoot densities (number of shoots/ m^2) and dried shoot weight ($\text{g}/\text{number of shoots}$) of the clipped quadrats (drying at 70°C for 72h) (Pérez-Harguindeguy et al., 2013). Before drying the harvested samples, the shoot length was measured and pictures were made to calculate the frontal area of the entire plants. Therefore, above-ground plant material was spread on a white background to make high contrast pictures (>8 Mega pixels). Using ArcMap (Environmental Systems Research Institute (ESRI), ArcGIS release 10.3, Redlands, CA) the surface area was determined through an Iso Cluster Unsupervised classification. This process was automated with a Python code.

2.6.2. Stem biomechanical traits

Mechanical properties of the lowest 0.20 m of the stems were measured with a three-point bending test at the Royal Netherlands Institute of Sea Research (NIOZ). The measuring method and calculations are based on Usherwood et al. (1997) and Silinski et al. (2016). The universal testing machine Instron EMSYSL7049 (precision $\pm 0.5\%$) with a 10 kN load cell was used (Instron Corporation, Canton, MA, USA). Force was applied at a displacement rate of 10 mm min^{-1} to the centre of a 0.20 m long stem section resting on two supports. The supports are separated from each other at a distance of 15 times the stem diameter which reduces the effect of shear stress (Usherwood et al., 1997). From the resulting stress-strain curve the Young's modulus (E in N/m^2) was calculated based on the slope of the elastic deformation zone, as a measure of the stress that can be applied on the stem before permanent deformation occurs (i.e. before the stem breaks). Higher values for Young's modulus mean lower flexibility of the stems. Second moment of area (I in m^4) was calculated based on a triangular stem geometry for *B. maritimus* $I = bh^3/36$ and based on a round stem geometry for *S. tabernaemontani* $I = \pi r^4/64$ where b is the base and h is the height of

the triangular cross section, and r is the diameter of the circular cross section (m). The flexural stiffness or stem flexibility, which is a measure of the resistance of the stem against breaking, was then calculated as EI (Nm^2). Higher values for flexural stiffness indicate higher stiffness and therefore lower flexibility. The stress experienced by the plants can be expressed by the drag forces acting on the shoots. Drag forces could not be measured directly in the field but proxies were used to give an idea of the relative differences between drag forces experienced by the two species. From the Morison equation adapted by Vogel (1996) we used the frontal plant area and flexural stiffness as proxies for drag force F (N):

$$F = \frac{1}{2} \rho a A v U^{2+d} \quad \text{Eq. (1)}$$

where ρ is the density of the fluid [kg m^{-3}], A is the wet frontal area of the shoot [m^2] and a and d are the species-specific constants that depend on the flexibility of the plant shoot.

2.7. Data analysis

Statistical analyses were performed in R 3.3.1. (R Core Team, 2016) and significance was assumed at $p < 0.05$ for all tests (exceptions are indicated). Normality was tested based on visual inspection with histograms and Q-Q plots and homogeneity of variance was tested with the F-test where needed. The species comparison was done with the Welch two sample t -test when the data was normally distributed or the unpaired two-sample Wilcoxon rank sum test (also named Mann-Whitney U test) for non-parametric data which both take into account the different origins (marsh sites) of the samples. The hydrodynamics in both species zones were compared using linear mixed models with time as a random factor.

3. Results

3.1. Plant zonation

The elevation distribution of *S. tabernaemontani* lies lower in the tidal frame compared to *B. maritimus*. This observation was consistent in the present study sites and in both the Elbe and Weser estuaries (Fig. 4).

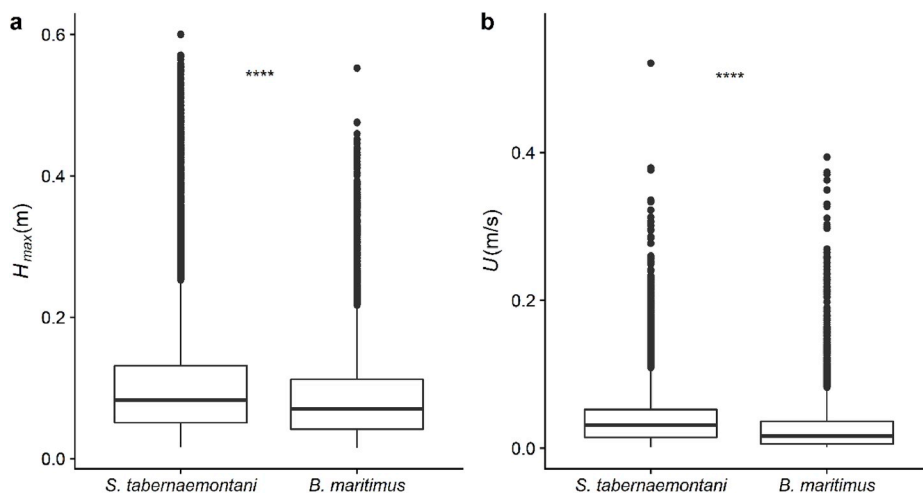


Fig. 5. The boxplots show the maximum wave height (H_{max} ; m) calculated over 10 min time intervals ($n = 96552$ and $n = 80410$ for the *S. tabernaemontani* and *B. maritimus* zones respectively) and planar flow velocity (U ; m/s) averaged over 10 min time intervals for the two pioneer species during the growing season from May to October 2016 ($n = 9629$ and $n = 7020$ for *S. tabernaemontani* and *B. maritimus* respectively). Incoming wave heights and flow velocities for *S. tabernaemontani* were significantly higher compared to *B. maritimus*. Flow velocities were solely measured at the site Hollerwettern due to limited sensor availability. Significance of differences was tested with the non-parametric Wilcoxon test (**** represents $p < 0.001$).

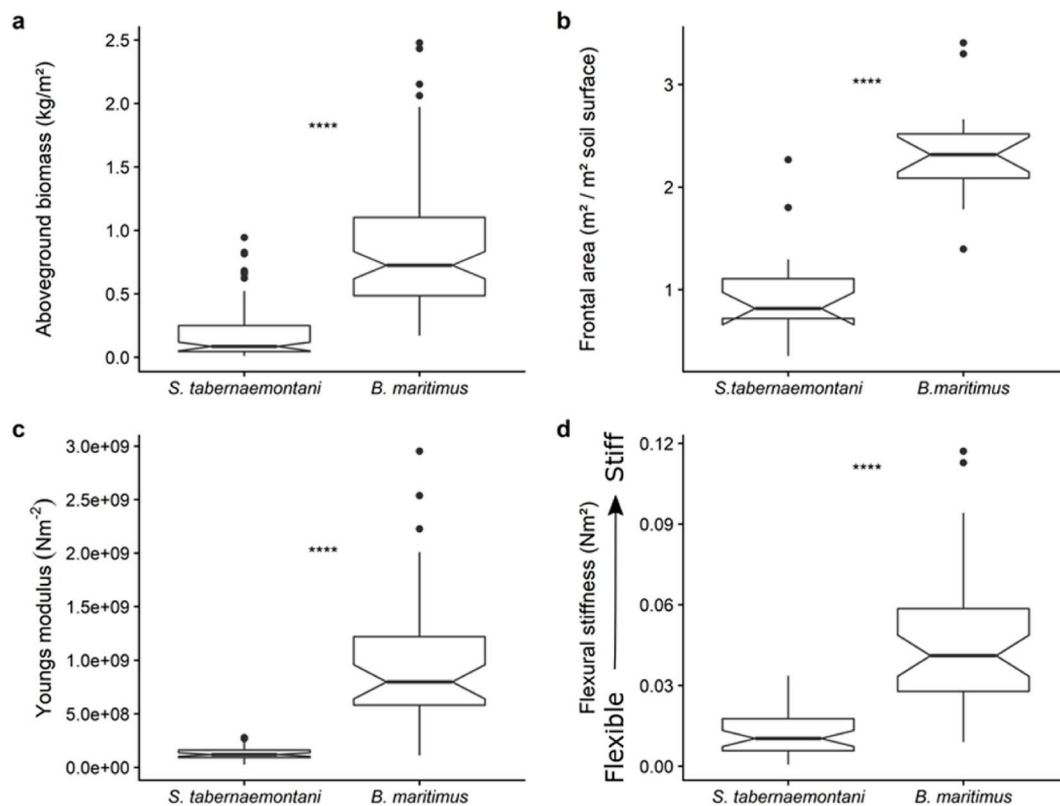


Fig. 6. Aboveground biomass (kg/m^2) (a) and frontal area (m^2/m^2 soil surface) (b) show the shoot morphological traits and Young's modulus (N/m^2) (c) and flexural stiffness (Nm^2) (d) show the stem biomechanical traits. All traits are represented in boxplots as a descriptive statistic per species at peak biomass in summer 2016 ($n = 83$ for a, 16 for b and $n = 40$ for c and d). Significance of differences was tested with the non-parametric Wilcoxon test (**** represents $p < 0.001$).

S. tabernaemontani grows in the small fringe between the mean water level and the *B. maritimus* zone.

3.2. Hydrodynamic forces of the *S. tabernaemontani* and *B. maritimus* zones

S. tabernaemontani is exposed to stronger hydrodynamic forces as compared to *B. maritimus* (Fig. 5). During the growing season of 2016, peak values for the maximum wave heights over 10 min intervals were found to be up to 0.5 m in the *B. maritimus* zone and up to 0.6 m in the *S. tabernaemontani* zone (Chi-square (1) = 54.18, $p < 0.001$). The median incoming significant wave height was 0.06 m in the *B. maritimus*

zone and 0.08 m in the *S. tabernaemontani* zone which was up to 25% higher (Chi-square (1) = 20623, $p < 0.001$; not shown in the figure). This difference in incoming wave heights is consistent over the measurement period (see Supplementary Fig. S2 for a time series). Median planar flow velocity in Hollerwettern was 0.025 ms^{-1} in the *B. maritimus* zone and 0.040 ms^{-1} in the *S. tabernaemontani* zone (Chi-square (1) = 534.42, $p < 0.001$). The 99th percentile of planar flow velocities reached 0.16 ms^{-1} in *B. maritimus* and 0.19 ms^{-1} in *S. tabernaemontani*. The different exposure to hydrodynamic forces was found consistent over the different elevation gradients of both study sites (see Fig. S1 in supplementary info).

Table 1

Overview of the plant traits measured for both *S. tabernaemontani* and *B. maritimus*. Per species, the mean and standard error are given in addition to the p-value of the Wilcoxon rank sum test which indicates the difference between the two species. The variables presented are aboveground dry biomass (AGB kg/m²), frontal area per soil surface area (FA, m²/m²) and frontal area per shoot (FA_{sh}, m²/shoot), Young's modulus (E, N/m²) and Flexural stiffness (EI, Nm²).

	AGB (kg/m ²)	FA (m ² / m ²)	FA _{sh} (m ² / shoot)	E (N/ m ²)	EI (Nm ²)
<i>S. tabernaemontani</i>	0.19 ± 0.02	0.99 ± 0.13	3e-3 ± 4e-4	1.3e8 ± 9e6	0.013 ± 0.001
<i>B. maritimus</i>	0.89 ± 0.06	2.34 ± 0.13	8e-3 ± 4e-4	9.7e8 ± 1e8	0.047 ± 0.004
p-value	<0.001	<0.001	<0.001	<0.001	<0.001

3.3. Plant species traits

The two species show different plant traits measured at peak biomass in August 2016. This trend is visible at both study sites. The aboveground dry biomass (AGB) of *S. tabernaemontani* is more than seven times smaller compared to *B. maritimus* (Fig. 6a, Table 1). In addition, *S. tabernaemontani* produces less frontal area compared to *B. maritimus*, both per soil surface area and per shoot (Fig. 6b, Table 1). The shoot tissue of *S. tabernaemontani* is more flexible, i.e. low Young's modulus, and less resistant against bending, i.e. low flexural stiffness, compared to *B. maritimus* (Fig. 6c and 6d, Table 1).

3.4. Species-dependent attenuation of hydrodynamic forces

Attenuation rates of waves and flow velocities were compared for the same water depth classes (Fig. 7). Especially for the shallow water depths, wave attenuation was stronger in the *B. maritimus* zone. With increasing water depth, wave attenuation decreased in both species zones. Moreover, the difference between the species-zones reduces when water depths increased. Yet for all water depth classes the differences in attenuation rates between both species-zones were statistically significant (Fig. 7). In the *S. tabernaemontani* zone, the wave attenuation rate dropped to almost zero at a water depth higher than 1.5 m. Planar flow attenuation rates were significantly higher in *B. maritimus* compared to *S. tabernaemontani*. In contrast to the wave attenuation, the flow attenuation did not change with increasing water depth (Fig. 7). For water depths over 1.5 m (not shown in Fig. 7) no significant difference in flow attenuation rate between both species was found which might be attributed to the low sample size (n = 14).

In the set-up of this study (Fig. 3), *S. tabernaemontani* grows in front of *B. maritimus* so that incoming wave heights in the *B. maritimus* zone

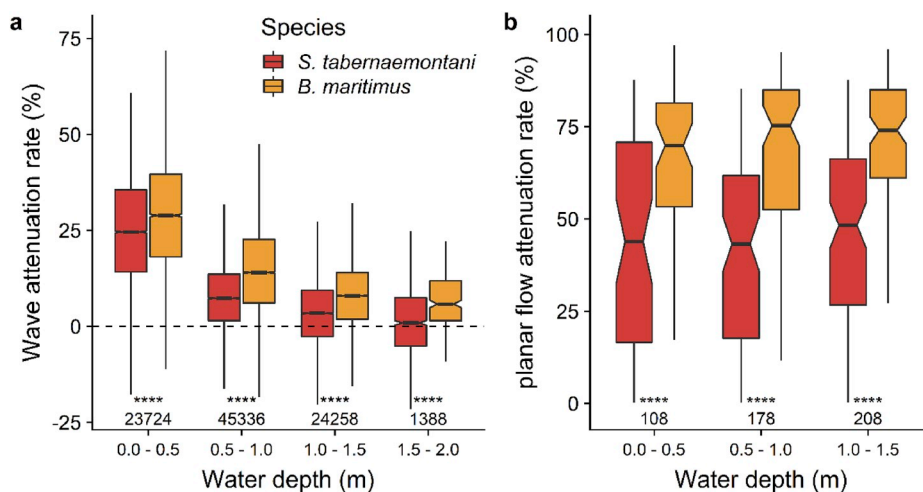


Fig. 7. Boxplots of wave and planar flow attenuation rates over 10 m stretches of *S. tabernaemontani* and *B. maritimus* measured during peak biomass (August 2016). Wave attenuation rates (number of measurements is indicated per water depth) and flow attenuation rate (n is indicated per water depth, for water depths >1.5 m the number of data points was too low and therefore data are not shown) are grouped per class of water depth. Significance of differences was tested with the non-parametric Wilcoxon test (**** represents p < 0.001).

are affected by wave transformation in front of that vegetation zone, i.e. within the *S. tabernaemontani* zone. In order to compare the wave attenuation rates of both the *S. tabernaemontani* and *B. maritimus* zones, we therefore compared wave attenuation rates for categories of the same incoming wave heights. Within each incoming wave height category, we find then that there is a significantly higher wave height attenuation rate within the *B. maritimus* zone as compared to the *S. tabernaemontani* zone (Fig. 8).

4. Discussion

Nature-based mitigation of coastal flood and erosion risks is increasingly studied in the context of growing risks associated with global and local changes, and in light of growing demand for novel, sustainable risk mitigation strategies (Duarte et al., 2013; Cheong et al., 2013; Temmerman et al., 2013; Vuik et al., 2016). Accordingly, conservation and restoration of tidal marshes that contribute to wave, flow

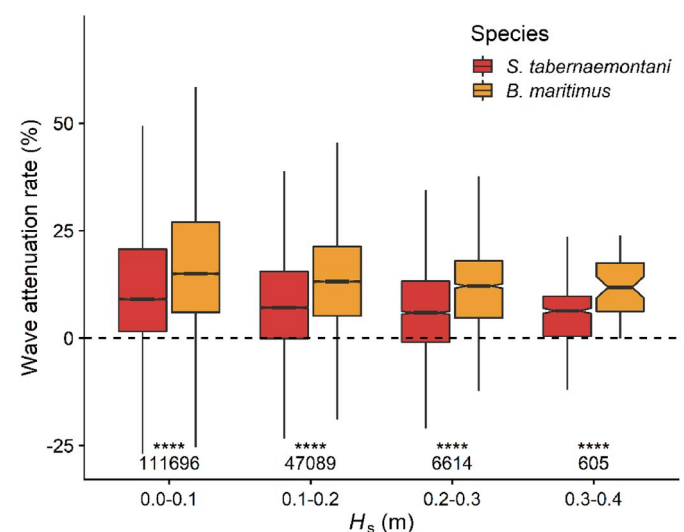


Fig. 8. Boxplots of wave attenuation rates over 10 m stretches of *S. tabernaemontani* and *B. maritimus* measured during the growing season (May 2016–October 2016). Wave attenuation rates (n is indicated per H_s class of 0.10 m) are grouped in classes of significant wave heights entering the specific vegetation zone. This allows a comparison of wave attenuation rates for both species zones independent of their location/distance from the marsh edge. Significance of differences was tested with the non-parametric Wilcoxon test (**** represents p < 0.001).

and erosion reduction, is increasingly proposed and implemented (Narayan et al., 2016; Gracia et al., 2018; Rangel-buitrago et al., 2018). A large amount of studies have focused on how plant species traits determine the effectiveness of wave, flow and erosion reduction (Bouma et al., 2005, 2010; Yang et al., 2012; Tempest et al., 2015; Carus et al., 2016), while fewer knowledge exists on how species traits determine their capacity to cope with and grow under wave and flow conditions (Coops and Van der Velde, 1996; Heuner et al., 2015; Silinski et al., 2017). Here we demonstrate under field conditions that plant species zonation is associated with trade-offs between species traits that allow coping with wave and flow exposure versus attenuation of these hydrodynamic forces (Fig. 6 and 7): (1) pioneer species growing at the exposed marsh front have plant traits that are better suited to avoid wave and current-induced stress compared to species growing more landward; (2) the same plant traits induce less effective attenuation of hydrodynamic forces in the exposed marsh front zone as compared to the more landward marsh zone. In the following, the trade-off involving species specific plant traits and hydrodynamic forces will be discussed more in details.

4.1. Avoidance capacity of species-specific plant traits

S. tabernaemontani and *B. maritimus* are pioneer plant species in brackish tidal marshes that grow in a similar elevation range, yet often in separate spatial zones, with *S. tabernaemontani* growing in the zone directly adjacent to the marsh front and *B. maritimus* in a more landward zone (Heuner et al., 2018, Fig. 4). Under exposed conditions we found that incoming wave heights and flow velocities were higher in the *S. tabernaemontani* zone compared to the *B. maritimus* zone independently from site elevation, distance from the marsh edge or incoming wave height (Figs. 4 and 8). The results show that on local scales the capacity to cope with such hydrodynamic forces is plant trait dependent. Under strong mechanical stress, plants are more vulnerable to mechanical failure such as uprooting, toppling and even breaking of the stem (Read and Stokes, 2006). Therefore, plants developed morphological and biomechanical adaptations (amongst others) (Albayrak et al., 2012; Puijalon and Bornette, 2013). *S. tabernaemontani* has a simple morphology of a single leafless stem creating vegetation with low biomass per square meter (Figs. 1 & 6). Especially the lack of leaves reduces the frontal area which is important to minimize the drag experienced by the plant (e.g. up to 60%, Bal et al., 2011).

In addition to the simple morphology, *S. tabernaemontani* has more flexible shoot bases (Fig. 6) which allows it to bend with passing waves or tidal currents. This flexibility enables the plants to reduce the experienced drag forces even more (Puijalon et al., 2005; Paul et al., 2016). Since drag forces were not measured directly in the field, the proxies used in this study (frontal plant area, flexural stiffness) indicate that drag forces exerted on *S. tabernaemontani* should be lower than on *B. maritimus* (Rupprecht et al., 2015). In terrestrial (wind driven) ecosystems however, some authors point out that high flexibility could increase the experienced drag as a result of the so-called flagging of the plant and turbulent flows created (Anten and Sterck, 2012; Butler et al., 2012). Nevertheless, they stress that under hydrodynamic forces a turbulent flow regime is less likely to fully develop as a result of lower flow velocities and the higher density of water compared to air. The morphological and biomechanical traits of *S. tabernaemontani* favor an efficient avoidance of mechanical stress. This may allow them to grow directly adjacent to the marsh front under the prevailing hydrodynamic forces (Henry et al., 2015; Paul and Gillis, 2015).

In contrast, *B. maritimus* grows leaves along the full length of the stem and thus produces high biomass with a high frontal area (Figs. 1 & 6). The morphological traits of *B. maritimus* results in higher drag forces which make them more vulnerable to mechanical failure if they would grow under high wave and current exposure. The biomechanical traits measured for *B. maritimus* and *S. tabernaemontani* were in the same range of values found in literature (Silinski et al., 2015, 2016; Vuik et al.,

2018). The flexural stiffness of *S. tabernaemontani* was 4–5 times smaller compared to values for *B. maritimus* (Fig. 6). The consequence of the stiffer shoots is that they do not reconfigure by elastic deformation to avoid the mechanical stress. Instead, they experience even more drag forces by keeping their rigid standing shoots (Bouma et al., 2005). Consequently, the growth of *B. maritimus* might be more limited by hydrodynamic forces, compared to *S. tabernaemontani*, which may be the reason why the first species grows landwards in more sheltered conditions. The ability to cope with hydrodynamic forces from waves and currents may thus be considered as a driver for species distribution (spatial zonation) along the sea-to-land gradient in pioneer tidal marshes. Although there is no experimental data available so far, future research with e.g. translocation experiments could give empirical proof for this mechanism. By growing both species under the same exposed and sheltered hydrodynamic conditions, insights on the survival chances of the species under the prevailing hydrodynamic conditions can be gained. Combining field data on plant survival chances and shoreline protection capacity of species in a model, could enable to make large scale (e.g. estuarine scale) assessments on the suitability of different intertidal areas for marsh restoration or conservation projects aiming at nature-based shoreline protection. This upscaling of the shoreline protection potential of an area is especially crucial for policy makers and environmental management agencies.

4.2. Wave and flow attenuation capacity of species-specific plant traits

As pointed out above, the two different species exert different frictions on the water motion and by this, attenuate rate of wave heights and current velocities in contrasting ways. When friction with the vegetation increases, the wave and flow attenuation becomes higher (Möller, 2006; Suzuki et al., 2012; Paul et al., 2016). *S. tabernaemontani* did not attenuate waves and water flows as much as *B. maritimus* did (Fig. 7) due to differences of the morphological and biomechanical properties of the two species (Fig. 6). High shoot stiffness and high shoot density are mentioned as the main drivers for wave attenuation (Feagin et al., 2011; Shepard et al., 2011), however biomass should be taken into account (Bouma et al., 2010; Ysebaert et al., 2011). The biomass per square meter accounts for both the shoots density and morphological properties of the shoots (e.g. stems, leaves, flowers). Nevertheless, when stems are highly flexible and bend away with passing waves and water flow, the effective biomass and frontal plant area under hydrodynamic forcing is reduced (Verschoren et al., 2016). Therefore, both stem flexibility and standing biomass are important drivers of the wave and flow attenuation capacity of a species. In general, species that avoid the mechanical stress, such as *S. tabernaemontani* will have a less effect on attenuation of hydrodynamic forces compared to species that resist the mechanical stress such as *B. maritimus*. It can be argued that the presented wave attenuation rates of *B. maritimus* are higher than for *S. tabernaemontani* because of the smaller incoming waves and lower water depths, and additionally several studies showed that the wave attenuation capacity of tidal marshes is strongest in the first few meters (Möller and Spencer, 2002; Koch et al., 2009; Carus et al., 2016). Nevertheless, we showed that under similar water depths (Fig. 7) and wave heights (Fig. 8) the wave attenuation rates in *B. maritimus* are consequently higher. This result shows that the difference in attenuation capacity is mainly caused by the difference in vegetation properties.

4.3. Avoiding or attenuating hydrodynamic forces: a trade-off

Based on our results, we formulate a conceptual model describing the trade-offs between coping with and attenuating hydrodynamics (Fig. 9). This means that species that can cope with hydrodynamic stress such as *S. tabernaemontani* have plant traits that limit the drag forces exerted on the plant, which in consequence results in a lesser attenuation capacity. However, landwards of such species, the hydrodynamic conditions become more favourable for other species that have a lower capacity to

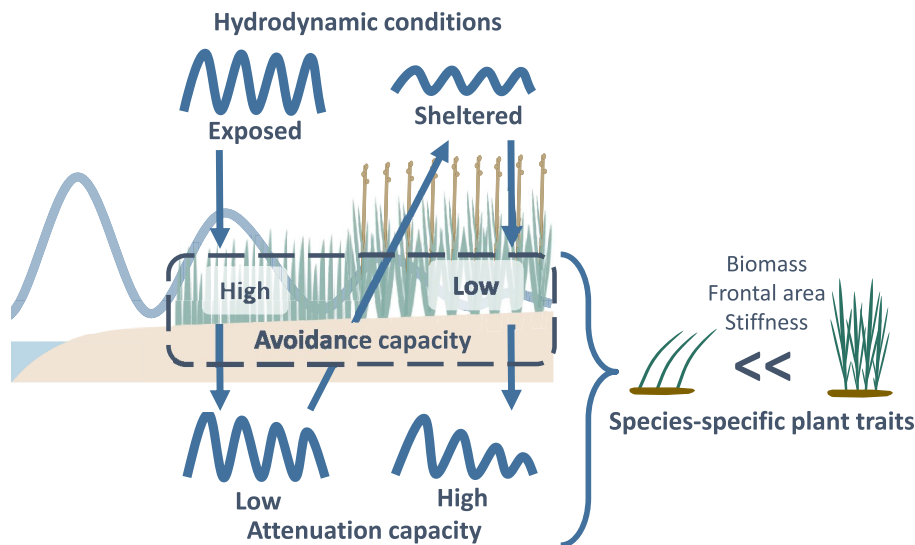


Fig. 9. Schematisation of the relationships between spatial plant species zonation, hydrodynamic forces in which the species grow, plant traits of the species, and the trade-off between the plants' capacity to avoid and to attenuate the hydrodynamic forces. Pioneer species growing at the marsh front are exposed to the strongest hydrodynamics. Accordingly, they have a high capacity to avoid mechanical stress as a result of species-specific plant traits that reduce the drag forces exerted on the shoot. As a consequence of these plant traits, the wave attenuation capacity of such species is low. The slightly sheltered conditions that are created more landward facilitate the growth of other species which have a lower capacity to cope with strong hydrodynamic stress. Corresponding species-specific plant traits result in higher drag forces, hence creating a stronger hydrodynamic attenuation capacity.

avoid the hydrodynamic stress due to their plant traits (e.g. *B. maritimus*). Such plant traits enhance the attenuation capacity of the species. In other words, avoiding the hydrodynamic stress reduces the attenuation capacity, but allows plants to grow in more hydrodynamic conditions. While in contrast, species that have less avoidance capacity enhance their attenuation capacity, but limit the hydrodynamic exposure that these species can handle to survive. *B. maritimus* has a higher ecosystem engineering capacity compared to *S. tabernaemontani* (Heuner et al., 2015) which gives them a competitive advantage when conditions are mild enough for their establishment and survival (Wilson and Keddy, 1986; Keddy, 2001; Heuner et al., 2018). When hydrodynamic forces limit the expansion of the *B. maritimus* zone, *S. tabernaemontani* might still be able to grow out in front of the *B. maritimus* zone. This is only possible when there is enough space for *S. tabernaemontani* to grow, which is often not the case and might force *S. tabernaemontani* into a stressful situation of both seaward stress coming from hydrodynamic forces and inundation stress as well as landward stress coming from competition with *B. maritimus*. Consequently, the trade-off between attenuation capacity and mechanical stress resistance presented in this field study might eventually create a zonation of species in exposed pioneer tidal marshes. Nevertheless, caution is needed as this study is descriptive and based on field observations, hence further experimental evidence is needed to come to causal conclusions.

4.4. Implications for natural shoreline protection

The trade-off described in this paper (Fig. 9) has consequences for bringing nature-based shoreline protection into practice: when conservation or restoration/creation of tidal marshes are proposed for shoreline protection, conditions might be unsuitable for the species that provide most efficient attenuation of hydrodynamic forces. In such case, shoreline protection capacity (here attenuation of hydrodynamics) is determined by the plant traits of the species that are able to grow under the prevailing hydrodynamic conditions. Hence, artificially creating slightly sheltered conditions (e.g. small man-made reefs in front of the shore or shallow willow fences) might facilitate the establishment and growth of species with a higher hydrodynamic attenuation capacity (e.g. *B. maritimus*) in an environment that normally would have been too exposed for such species. Nevertheless, the establishment of species that are able to cope with hydrodynamic exposure (e.g. *S. tabernaemontani*) can result already in some degree of wave attenuation and therefore can naturally create these slightly sheltered conditions where growth of other, less wave tolerant species can be facilitated. Provided that there is

enough space (perpendicular to the dike/shipping channel) to allow the development of such a species zonation in the pioneer zones of marshes, the overall efficiency of shoreline protection will increase as the result of this natural species zonation.

Declaration of competing interest

The authors declare that they have no known competing financial interests or personal relationships that could have appeared to influence the work reported in this paper.

CRediT authorship contribution statement

Ken Schoutens: Conceptualization, Methodology, Validation, Formal analysis, Investigation, Writing - original draft, Writing - review & editing, Visualization. **Maïke Heuner:** Conceptualization, Methodology, Validation, Formal analysis, Resources, Writing - review & editing, Funding acquisition, Project administration, Supervision. **Elmar Fuchs:** Conceptualization, Methodology, Validation, Writing - review & editing. **Vanessa Minden:** Conceptualization, Methodology, Validation, Writing - review & editing. **Tilla Schulte-Ostermann:** Conceptualization, Methodology, Validation, Writing - review & editing. **Jean-Philippe Belliard:** Validation, Formal analysis, Writing - review & editing. **Tjeerd J. Bouma:** Validation, Resources, Writing - review & editing. **Stijn Temmerman:** Conceptualization, Methodology, Validation, Resources, Writing - review & editing, Funding acquisition, Supervision.

Acknowledgements

We would like to thank Wasserstraßen-und Schifffahrtsamt Hamburg (Glückstadt, Germany) for logistical support in the field; Hannes Sahl and Thomas Jansen for measuring the elevations with dGPS; Niels Van Putte for providing the Python code; Flanders Hydrology for providing the Matlab routine to process the wave data and all field assistants for occasional help. This research was financed by the research project TIBASS (Tidal Bank Science and Services) of the Bundesanstalt für Gewässerkunde (Bfg), Koblenz, Germany and the Research Foundation Flanders, Belgium (FWO, PhD fellowship for fundamental research K. Schoutens, 1116319N).

Appendix A. Supplementary data

Supplementary data to this article can be found online at <https://doi.org/10.1016/j.ecss.2020.106645>.

[org/10.1016/j.ecss.2020.106645](https://doi.org/10.1016/j.ecss.2020.106645).

References

- Albayrak, I., Nikora, V., Miler, O., O'Hare, M., 2012. Flow-plant interactions at a leaf scale: effects of leaf shape, serration, roughness and flexural rigidity. *Aquat. Sci.* 74, 267–286. <https://doi.org/10.1007/s00027-011-0220-9>.
- Anderson, M.E., Smith, J.M., 2014. Wave attenuation by flexible, idealized salt marsh vegetation. *Coast. Eng.* 83, 82–92. <https://doi.org/10.1016/j.coastaleng.2013.10.004>.
- Anderson, M.E., Smith, J.M., McKay, S.K., 2011. Wave Dissipation by Vegetation. Coastal and Hydraulics Engineering Technical Note ERDC/CHL CHETN-1-82. Vicksburg, MS US Army Corps Eng. Eng. Res. Dev. Center., p. 22.
- Anten, N.P.R., Sterck, F.J., 2012. Terrestrial vs aquatic plants: how general is the drag tolerance-avoidance trade-off? *New Phytol.* 193, 6–8. <https://doi.org/10.1111/j.1469-8137.2011.03994.x>.
- Anten, Niels P.R., Casado-García, Nagashima, 2017. Effects of mechanical stress and plant density on mechanical characteristics, growth, and lifetime reproduction of tobacco plants. *Am. Nat.* 166, 650. <https://doi.org/10.2307/3491228>.
- Auerbach, L.W., Goodbred, S.L., Mondal, D.R., et al., 2015. Flood risk of natural and embanked landscapes on the Ganges-Brahmaputra tidal delta plain. *Nat. Clim. Change* 5, 153–157. <https://doi.org/10.1038/nclimate2472>.
- Bal, K.D., Bouma, T.J., Buis, K., Struyf, E., Jonas, S., Backx, H., Meire, P., 2011. Trade-off between drag reduction and light interception of macrophytes: comparing five aquatic plants with contrasting morphology. *Funct. Ecol.* 25, 1197–1205. <https://doi.org/10.1111/j.1365-2435.2011.01909.x>.
- Belliard, J.P., Silinski, A., Meire, D., Kolokythas, G., Levy, Y., Van Braeckel, A., Bouma, T. J., Temmerman, S., 2019. High-resolution bed level changes in relation to tidal and wave forcing on a narrow fringing macrotidal flat: bridging intra-tidal, daily and seasonal sediment dynamics. *Mar. Geol.* 412, 123–138. <https://doi.org/10.1016/j.margeo.2019.03.001>.
- Biddington, N.L., 1986. The effects of mechanically-induced stress in plants - a review. *Plant Growth Regul.* 4, 103–123. <https://doi.org/10.1007/BF00025193>.
- Bouma, T.J., De Vries, M.B., Low, E., Peralta, G., Tanczos, I.C., van de Koppel, J., Herman, P.M.J., 2005. Trade-offs related to ecosystem engineering: a case study on stiffness of emerging macrophytes. *Ecology* 86, 2187–2199. <https://doi.org/10.1890/04-1588>.
- Bouma, T.J., Friedrichs, M., van Wesenbeeck, B.K., Brun, F.G., Temmerman, S., de Vries, M.B., Graf, G., Herman, P.M.J., 2008. Plant growth strategies directly affect biogeomorphology of estuaries. In: *River, Coastal and Estuarine Morphodynamics: RCEM 2007, Two Volume Set*, p. 292.
- Bouma, T., Friedrichs, M., Klaassen, P., et al., 2009. Effects of shoot stiffness, shoot size and current velocity on scouring sediment from around seedlings and propagules. *Mar. Ecol. Prog. Ser.* 388, 293–297. <https://doi.org/10.3354/meps08130>.
- Bouma, T.J., De Vries, M.B., Herman, P.M.J., 2010. Comparing ecosystem engineering efficiency of two plant species with contrasting growth strategies. *Ecol. Soc. Am.* 91, 2696–2704. <https://doi.org/10.1890/09-0690.1>.
- Bouma, T.J., van Belzen, J., Balke, T., et al., 2014. Identifying knowledge gaps hampering application of intertidal habitats in coastal protection: opportunities & steps to take. *Coast. Eng.* 87, 147–157. <https://doi.org/10.1016/j.coastaleng.2013.11.014>.
- Butler, D.W., Gleason, S.M., Davidson, I., Onoda, Y., Westoby, M., 2012. Safety and streamlining of woody shoots in wind: an empirical study across 39 species in tropical Australia. *New Phytol.* 193, 137–149. <https://doi.org/10.1111/j.1469-8137.2011.03887.x>.
- Callaghan, D.P., Bouma, T.J., Klaassen, P., van der Wal, D., Stive, M.J.F., Herman, P.M.J., 2010. Hydrodynamic forcing on salt-marsh development: distinguishing the relative importance of waves and tidal flows. *Estuar. Coast Shelf Sci.* 89, 73–88. <https://doi.org/10.1016/j.ecss.2010.05.013>.
- Carus, J., Paul, M., Schröder, B., 2016. Vegetation as self-adaptive coastal protection: reduction of current velocity and morphologic plasticity of a brackish marsh pioneer. *Ecol. Evol.* 6, 1579–1589. <https://doi.org/10.1002/ece3.1904>.
- Chen, H., Ni, Y., Li, Y., et al., 2018. Deriving vegetation drag coefficients in combined wave-current flows by calibration and direct measurement methods. *Adv. Water Resour.* 122, 217–227. <https://doi.org/10.1016/j.advwatres.2018.10.008>.
- Cheong, S.-M., Silliman, B., Wong, P.P., van Wesenbeeck, B., Kim, C.-K., Guannel, G., 2013. Coastal adaptation with ecological engineering. *Nat. Clim. Change* 3, 787–791. <https://doi.org/10.1038/nclimate1854>.
- Coops, H., Van der Velde, G., 1996. Effects of waves on helophyte stands: mechanical characteristics of stems of *Phragmites australis* and *Scirpus lacustris*. *Aquat. Bot.* 53, 175–185. [https://doi.org/10.1016/0304-3770\(96\)01026-1](https://doi.org/10.1016/0304-3770(96)01026-1).
- Dalrymple, R.A., Dean, R.G., 1991. *Water Wave Mechanics for Engineers and Scientists*, vol. 2. Prentice-Hall.
- Denny, M.W., 1994. Extreme drag forces and the survival of wind- and water-swept organisms. *J. Exp. Bot.* 194, 97–115.
- Denny, M.W., Gaylord, B., 2002. Review the mechanics of wave-swept algae. *J. Exp. Biol.* 205, 1355–1362.
- Denny, M.W., Miller, L.P., Stokes, M.D., Hunt, L.J.H., Helmuth, B.S.T., 2003. Extreme water velocities: topographical amplification of wave-induced flow in the surf zone of rocky shores. *Limnol. Oceanogr.* 48, 1–8. <https://doi.org/10.4319/lo.2003.48.1.0001>.
- Duarte, C.M., Losada, I.J., Hendriks, I.E., Mazarrasa, I., Marbà, N., 2013. The role of coastal plant communities for climate change mitigation and adaptation. *Nat. Clim. Change* 3, 961–968. <https://doi.org/10.1038/nclimate1970>.
- DWD Climate Data Center, (CDC), 2019. Recent hourly station observations of wind speed and wind direction for Germany, quality control not completed yet. http://ft.p-cdc.dwd.de/Pub/CDC/Observations_germany/Climate/Hourly/.
- Feagin, R.A., Irish, J.L., Möller, I., Williams, a.M., Colón-Rivera, R.J., Mousavi, M.E., 2011. Short communication: engineering properties of wetland plants with application to wave attenuation. *Coast. Eng.* 58, 251–255. <https://doi.org/10.1016/j.coastaleng.2010.10.003>.
- Feagin, R.A., Furman, M., Salgado, K., et al., 2019. The role of beach and sand dune vegetation in mediating wave run up erosion. *Estuar. Coast Shelf Sci.* 219, 97–106. <https://doi.org/10.1016/j.ecss.2019.01.018>.
- Friess, D. a, Krauss, K.W., Horstman, E.M., Balke, T., Bouma, T.J., Galli, D., Webb, E.L., 2012. Are all intertidal wetlands naturally created equal? Bottlenecks, thresholds and knowledge gaps to mangrove and saltmarsh ecosystems. *Biol. Rev. Camb. Phil. Soc.* 87, 346–366. <https://doi.org/10.1111/j.1469-185X.2011.00198.x>.
- Gedan, K.B., Kirwan, M.L., Wolanski, E., Barbier, E.B., Silliman, B.R., 2011. The present and future role of coastal wetland vegetation in protecting shorelines: answering recent challenges to the paradigm. *Climatic Change* 106, 7–29. <https://doi.org/10.1007/s10584-010-0003-7>.
- Gracia, A., Rangel-Buitrago, N., Oakley, J.A., Williams, A.T., 2018. Use of ecosystems in coastal erosion management. *Ocean Coast Manag.* 156, 277–289. <https://doi.org/10.1016/j.ocecoaman.2017.07.009>.
- Hallegatte, S., Green, C., Nicholls, R.J., Corfee-Morlot, J., 2013. Future flood losses in major coastal cities. *Nat. Clim. Change* 3, 802–806. <https://doi.org/10.1038/nclimate1979>.
- Hamann, E., Puijalon, S., 2013. Biomechanical responses of aquatic plants to aerial conditions. *Ann. Bot.* 112, 1869–1878. <https://doi.org/10.1093/aob/mct221>.
- Henry, P.Y., Myrhaug, D., Aberle, J., 2015. Drag forces on aquatic plants in nonlinear random waves plus current. *Estuar. Coast Shelf Sci.* 165, 10–24. <https://doi.org/10.1016/j.ecss.2015.08.021>.
- Heuner, M., Silinski, A., Schoelynck, J., et al., 2015. Ecosystem engineering by plants on wave-exposed intertidal flats is governed by relationships between effect and response traits. *PloS One* 10, e0138086. <https://doi.org/10.1371/journal.pone.0138086>.
- Heuner, M., Schröder, B., Schröder, U., Kleinschmit, B., 2018. Contrasting elevational responses of regularly flooded marsh plants in navigable estuaries. *Ecohydrol. Hydrobiol.* 19, 38–53. <https://doi.org/10.1016/j.ecohyd.2018.06.002>.
- Keddy, P.A., 2001. Modelling competition chapter 9. In: *Competition*. Kluwer Academic Publishers, pp. 333–404.
- Koch, E.W., Barbier, E.B., Silliman, B.R., et al., 2009. Non-linearity in ecosystem services: temporal and spatial variability in coastal protection. *Front. Ecol. Environ.* 7, 29–37. <https://doi.org/10.1890/080126>.
- Leonard, L.A., Croft, A.L., 2006. The effect of standing biomass on flow velocity and turbulence in *Spartina alterniflora* canopies. *Estuar. Coast Shelf Sci.* 69, 325–336. <https://doi.org/10.1016/j.ecss.2006.05.004>.
- Miler, O., Albayrak, I., Nikora, V., O'Hare, M., 2012. Biomechanical properties of aquatic plants and their effects on plant-flow interactions in streams and rivers. *Aquat. Sci.* 74, 31–44. <https://doi.org/10.1007/s00027-011-0188-5>.
- Miler, O., Albayrak, I., Nikora, V., O'Hare, M., 2014. Biomechanical properties and morphological characteristics of lake and river plants: implications for adaptations to flow conditions. *Aquat. Sci.* <https://doi.org/10.1007/s00027-014-0347-6>.
- Möller, I., 2006. Quantifying saltmarsh vegetation and its effect on wave height dissipation: results from a UK East coast saltmarsh. *Estuar. Coast Shelf Sci.* 69, 337–351. <https://doi.org/10.1016/j.ecss.2006.05.003>.
- Möller, I., Spencer, T., 2002. Wave dissipation over macro-tidal saltmarshes: effects of marsh edge typology and vegetation change. *J. Coast Res.* 36, 506–521. <https://doi.org/10.2112/1551-5036-36.sp1.506>.
- Möller, I., Kudella, M., Rupprecht, F., et al., 2014. Wave attenuation over coastal salt marshes under storm surge conditions. *Nat. Geosci.* 7, 727–731. <https://doi.org/10.1038/ngeo2251>.
- Narayan, S., Beck, M.W., Reguero, B.G., et al., 2016. The effectiveness, costs and coastal protection benefits of natural and nature-based defences. *PloS One* 11, e0154735. <https://doi.org/10.1371/journal.pone.0154735>.
- Nepf, H.M., 1999. Drag, turbulence, and diffusion in flow through emergent vegetation. *Water Resour. Res.* 35, 479–489. <https://doi.org/10.1029/1998WR900069>.
- Nicholls, R.J., Hanson, S., Herweijer, C., Patmore, N., Hallegatte, S., Corfee-Morlot, J., Chateau, J., Muir-Wood, R., 2008. Ranking port cities with high exposure and vulnerability to climate extremes: exposure estimates. *OECD Environ. Work. Pap.* 1 <https://doi.org/10.1787/011766488208>.
- Paul, M., Gillis, L.G., 2015. Let it flow: how does an underlying current affect wave propagation over a natural seagrass meadow? *Mar. Ecol. Prog. Ser.* 523, 57–70. <https://doi.org/10.3354/meps11162>.
- Paul, M., Rupprecht, F., Möller, I., et al., 2016. Plant stiffness and biomass as drivers for drag forces under extreme wave loading: a flume study on mimics. *Coast. Eng.* 117, 70–78. <https://doi.org/10.1016/j.coastaleng.2016.07.004>.
- Pérez-Harguindeguy, N., Díaz, S., Garnier, E., et al., 2013. New handbook for standardised measurement of plant functional traits worldwide. *Aust. J. Bot.* 61, 167–234. <https://doi.org/10.1071/BT12225>.
- Pethick, J., Orford, J.D., 2013. Rapid rise in effective sea-level in southwest Bangladesh: its causes and contemporary rates. *Global Planet. Change* 111, 237–245. <https://doi.org/10.1016/j.gloplacha.2013.09.019>.
- Puijalon, S., Bornette, G., 2013. Multi-scale macrophyte responses to hydrodynamic stress and disturbances: adaptive strategies and biodiversity patterns. In: *Ecohydraulics: an Integrated Approach*, pp. 261–270.
- Puijalon, S., Bornette, G., Sagnes, P., 2005. Adaptations to increasing hydraulic stress: morphology, hydrodynamics and fitness of two higher aquatic plant species. *J. Exp. Bot.* 56, 777–786. <https://doi.org/10.1093/jxb/eri063>.

- Puijalon, S., Bouma, T.J., Van Groenendael, J., Bornette, G., 2008. Clonal plasticity of aquatic plant species submitted to mechanical stress: escape versus resistance strategy. *Ann. Bot.* 102, 989–996. <https://doi.org/10.1093/aob/mcn190>.
- Puijalon, S., Bouma, T.J., Douady, C.J., van Groenendael, J., Anten, N.P.R., Martel, E., Bornette, G., 2011. Plant resistance to mechanical stress: evidence of an avoidance-tolerance trade-off. *New Phytol.* 191, 1141–1149. <https://doi.org/10.1111/j.1469-8137.2011.03763.x>.
- R Core Team, 2016. *A Language and Environment for Statistical Computing*. R, Vienna, Austria.
- Rangel-buitrago, N., De Jonge, V.N., Neal, W., 2018. How to make integrated coastal erosion management a reality. *Ocean Coast Manag.* 156, 290–299. <https://doi.org/10.1016/j.ocecoaman.2018.01.027>.
- Read, J., Stokes, A., 2006. Plant biomechanics in an ecological context. *Am. J. Bot.* 93, 1546–1565. <https://doi.org/10.3732/ajb.93.10.1546>.
- Rupprecht, F., Möller, I., Evans, B., Spencer, T., Jensen, K., 2015. Biophysical properties of salt marsh canopies — quantifying plant stem flexibility and above ground biomass. *Coast. Eng.* 100, 48–57. <https://doi.org/10.1016/j.coastaleng.2015.03.009>.
- Rupprecht, F., Möller, I., Paul, M., et al., 2017. Vegetation-wave interactions in salt marshes under storm surge conditions. *Ecol. Eng.* 100, 301–315. <https://doi.org/10.1016/j.ecoleng.2016.12.030>.
- Sand-Jensen, K., 2003. Drag and reconfiguration of freshwater macrophytes. *Freshw. Biol.* 48, 271–283. <https://doi.org/10.1046/j.1365-2427.2003.00998.x>.
- Schipper, C.A., Vreugdenhil, H., De Jong, M.P.C., 2017. A sustainability assessment of ports and port-city plans : comparing ambitions with achievements. *Transp. Res. Part D* 57, 84–111. <https://doi.org/10.1016/j.trd.2017.08.017>.
- Schoelynck, J., Puijalon, S., Meire, P., Struyf, E., 2015. Thigmomorphogenetic responses of an aquatic macrophyte to hydrodynamic stress. *Front. Plant Sci.* 6, 1–7. <https://doi.org/10.3389/fpls.2015.00043>.
- Schoutens, K., Heuner, M., Minden, V., Schulte Ostermann, T., Silinski, A., Belliard, J.-P., Temmerman, S., 2019. How effective are tidal marshes as nature-based shoreline protection throughout seasons? *Limnol. Oceanogr.* 64, 1750–1762. <https://doi.org/10.1002/lno.11149>.
- Schulze, D., Rupprecht, F., Nolte, S., Jensen, K., 2019. Seasonal and spatial within - marsh differences of biophysical plant properties : implications for wave attenuation capacity of salt marshes. *Aquat. Sci.* <https://doi.org/10.1007/s00027-019-0660-1>.
- Shepard, C.C., Crain, C.M., Beck, M.W., 2011. The protective role of coastal marshes: a systematic review and meta-analysis. *PLoS One* 6. <https://doi.org/10.1371/journal.pone.0027374>.
- Silinski, A., Heuner, M., Schoelynck, J., et al., 2015. Effects of wind waves versus ship waves on tidal marsh plants: a flume study on different life stages of *Scirpus maritimus*. *PLoS One* 10, e0118687. <https://doi.org/10.1371/journal.pone.0118687>.
- Silinski, A., Heuner, M., Troch, P., et al., 2016. Effects of contrasting wave conditions on scour and drag on pioneer tidal marsh plants. *Geomorphology* 255, 49–62. <https://doi.org/10.1016/j.geomorph.2015.11.021>.
- Silinski, A., Schoutens, K., Puijalon, S., Schoelynck, J., Luyckx, D., Troch, P., Meire, P., Temmerman, S., 2017. Coping with waves: plasticity in tidal marsh plants as self-adapting coastal ecosystem engineers. *Limnol. Oceanogr.* 63, 799–815. <https://doi.org/10.1002/lno.10671>.
- Stark, J., Van Oyen, T., Meire, P., Temmerman, S., 2015. Observations of tidal and storm surge attenuation in a large tidal marsh. *Limnol. Oceanogr.* 60, 1371–1381. <https://doi.org/10.1002/lno.10104>.
- Starko, S., Martone, P.T., 2016. Evidence of an evolutionary-developmental trade-off between drag avoidance and tolerance strategies in wave-swept intertidal kelps (Laminariales, Phaeophyceae). *J. Phycol.* 52, 54–63. <https://doi.org/10.1111/jpy.12368>.
- Starko, S., Claman, B.Z., Martone, P.T., 2015. Biomechanical consequences of branching in flexible wave-swept macroalgae. *New Phytol.* 206, 133–140. <https://doi.org/10.1111/nph.13182>.
- Strotmann, T., 2014. *Deutsches Gewässerkundliches Jahrbuch, Elbegebiet Teil 3, Untere Elbe ab der Havelmündung*.
- Suzuki, T., Zijlema, M., Burger, B., Meijer, M.C., Narayan, S., 2012. Wave dissipation by vegetation with layer schematization in SWAN. *Coast. Eng.* 59, 64–71. <https://doi.org/10.1016/j.coastaleng.2011.07.006>.
- Temmerman, S., Kirwan, M.L., 2015. Building land with a rising sea: cost-efficient nature-based solutions can help to sustain coastal societies. *Science* 349, 588–589. <https://doi.org/10.1126/science.aac8312>.
- Temmerman, S., Meire, P., Bouma, T.J., Herman, P.M.J., Ysebaert, T., De Vriend, H.J., 2013. Ecosystem-based coastal defence in the face of global change. *Nature* 504, 79–83. <https://doi.org/10.1038/nature12859>.
- Tempest, J.A., Möller, I., Spencer, T., 2015. A review of plant-flow interactions on salt marshes: the importance of vegetation structure and plant mechanical characteristics. *Wiley Interdiscip. Rev. Water* 2, 669–681. <https://doi.org/10.1002/wat2.1103>.
- Tessler, Z.D., Vörösmarty, C.J., Grossberg, M., Gladkova, I., Aizenman, H., Syvitski, J.P.M., Foufoula-Georgiou, E., 2015. Profiling risk and sustainability in coastal deltas of the world. *Science* 349, 638–643. <https://doi.org/10.1126/science.aab3574> (80-).
- Usherwood, J.R., Ennos, R., Ball, D.J., 1997. Mechanical and anatomical adaptations in terrestrial and aquatic buttercups to their respective environments. *J. Exp. Bot.* 48, 1469–1475. <https://doi.org/10.1093/jxb/48.7.1469>.
- Vanlierde, E., Michiels, S., Vereycken, K., Hertoghs, R., Meire, D., Deschamps, M., Verwaest, T., Mostaert, F., 2011. *Onderzoek naar de invloedsfactoren van golfbelasting en de morfologische effecten op slikken en schorren in de Beneden Zeeschelde, meer specifiek op het Galgeschoor: Deelrapport 2: Verslag testmeting van 29/11/2010 - 01/12/2010*. Technical Report. Waterb.
- Verschoren, V., Meire, D., Schoelynck, J., Buis, K., Bal, K.D., Troch, P., Meire, P., Temmerman, S., 2016. Resistance and reconfiguration of natural flexible submerged vegetation in hydrodynamic river modelling. *Environ. Fluid Mech.* 16, 245–265. <https://doi.org/10.1007/s10652-015-9432-1>.
- Vogel, S., 1996. *Life in Moving Fluids: the Physical Biology of Flow*, second ed. Princeton University Press.
- Vuik, V., Jonkman, S.N., Borsje, B.W., Suzuki, T., 2016. Nature-based flood protection: the efficiency of vegetated foreshores for reducing wave loads on coastal dikes. *Coast. Eng.* 116, 42–56. <https://doi.org/10.1016/j.coastaleng.2016.06.001>.
- Vuik, V., Suh Heo, H.Y., Zhu, Z., Borsje, B.W., Jonkman, S.N., 2018. Stem breakage of salt marsh vegetation under wave forcing: a field and model study. *Estuar. Coast Shelf Sci.* 200, 41–58. <https://doi.org/10.1016/j.ecss.2017.09.028>.
- Wilson, S.D., Keddy, P.A., 1986. Species competitive ability and position along a natural stress/disturbance gradient. *Ecology* 67, 1236–1242. <https://doi.org/10.2307/1938679>.
- Woodruff, J.D., Irish, J.L., Camargo, S.J., 2013. Coastal flooding by tropical cyclones and sea-level rise. *Nature* 504, 44–52. <https://doi.org/10.1038/nature12855>.
- WSA, H., 2017. *Außenelbe Nordsee und Tideelbe | DGM-W 2016 | verschiedene Teilgebiete. Modelldaten*.
- Yang, S.L., Shi, B.W., Bouma, T.J., Ysebaert, T., Luo, X.X., 2012. Wave attenuation at a salt marsh margin : a case study of an exposed coast on the Yangtze Estuary. *Estuar. Coast* 35, 169–182. <https://doi.org/10.1007/s12237-011-9424-4>.
- Ysebaert, T., Yang, S., Zhang, L., He, Q., Bouma, T.J., Herman, P.M.J., 2011. Wave attenuation by two contrasting ecosystem engineering salt marsh macrophytes in the intertidal pioneer zone. *Wetlands* 31, 1043–1054. <https://doi.org/10.1007/s13157-011-0240-1>.
- Zentrales Datenmanagement der GDWS Standort Kiel, W.H., 2017. *Digitale Orthophotos Unter- und Außenelbe (DOP020) WSA Hamburg 2016*.